Electronic Supplementary Material (ESI) for ChemComm.

Supporting Information

Diverse Macroscopic Helical Motions of Microribbons Driven by Electrons

Cheng Peng,[1,2,†] Yifan Zhang, [1,2,†] Yibin Zhang, [1,2,†] Zichao Zhou, [1,2] Yanke Che, [1,2,] and Jincai Zhao[1,2]*

[1]Key Laboratory of Photochemistry, Institute of Chemistry, Chinese Academy of Sciences, Beijing, 100080, China.
[2]University of Chinese Academy of Sciences, Beijing, 100049, China.
[†]These authors contributed equally to this work.

Materials.

All reagents and solvents were obtained from commercial suppliers and used as received unless otherwise noted.

Other supplies: Fisherfinest Premium Cover Glass (40×22×0.17 mm) purchased from Fisher Scientific. Filter membrane (Teflon 0.45 μm) purchased from PerkinElmer.

Synthesis of molecules I1, II1, and II2.

The synthesis of molecules **I1**, **II1**, and **II2** was performed following our previously reported procedure.[1] The pure compounds **I1** and **II1** were obtained by column chromatography (silica, chloroform: acetone =100:1) and confirmed by ^{1}HNMR and MALDI-TOF-MS as below. Although compound **II2** has poor solubility in all common organic solvent, it was still purified through column chromatography using chloroform as eluent and was confirmed by MALDI-TOF-MS as below.

Compound I1. ^{1}HNMR (400 MHz, $CDCl_3$): δ 8.71-8.74 (m, 4H), 8.63-8.70 (m, 4H), 7.57-7.60 (m, 1H), 7.31-7.35 (m, 4H), 5.42 (s, 2H), 4.18-4.23 (t, *J*= 20 Hz, 2H), 1.75-1.76 (m, 2H), 1.35-1.37 (t, *J*= 8 Hz, 6H), 1.25-1.27 (m, 18H), 0.86 (m, 3H); MALDI-TOF-MS: (m/z) = 648.5 (See Figures S10 and S11).

Compound II1. ^{1}HNMR (300 MHz, $CDCl_3$): δ 8.67-8.69 (m, 4H), 8.60-8.62 (m, 4H), 7.38-7.41 (m, 4H), 7.30-7.35 (m, 1H), 4,41-4.46 (m, 2H), 4.18-4.23 (t, *J* = 15 Hz, 2H), 3.04-3.09 (m, 2H), 1.74-1.79 (m, 2H), 1.25-1.27 (m, 18H), 0.82-0.89 (m, 9H); MALDI-TOF-MS: (m/z) = 662.4 (See Figures S14 and S15).

Compound II2. MALDI-TOF-MS: (m/z) = 570.2 (See Figure S16).

Synthesis of molecules I2, III and IV.

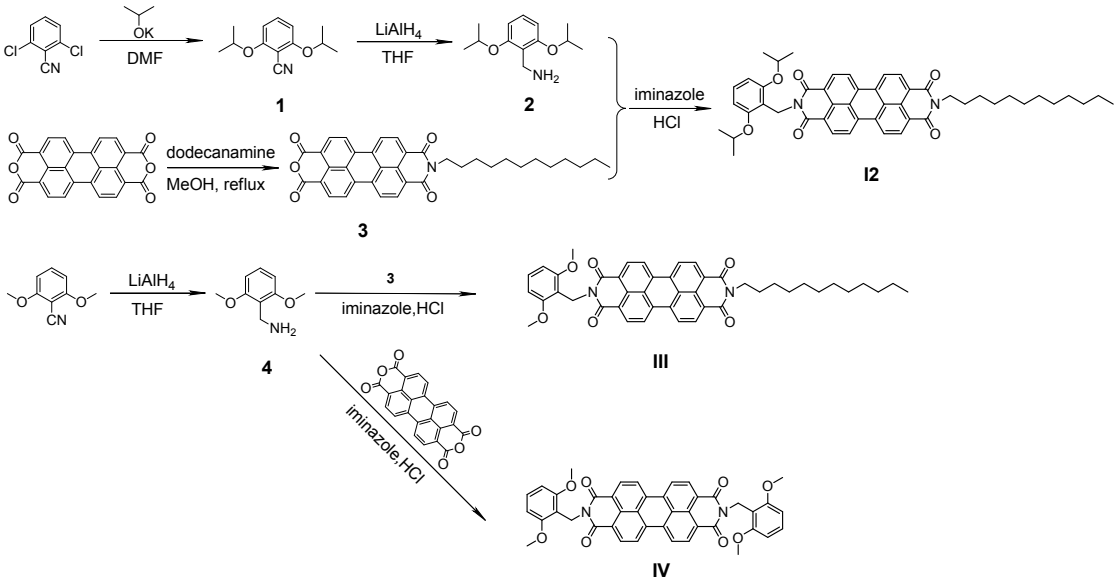

Scheme S1. The synthesis procedure of molecules **I2**, **III,** and **IV**.

Compound 1. A dimethyl formamide solution of 2,6-dichlorobenzonitrile (400 mg) and potassium isopropoxide (1.8 g, 8 mL) was heated to 180 °C and refluxed under argon overnight. After cooling to room temperature, the resulting solution was extracted with H_2O (20 mL) and then the water layer was extracted three times with ethyl acetate (3 × 10 mL). The combined organic layers were dried over sodium sulfate, and concentrated under vacuum. The residue was purified by column chromatography (silica, hexanes: ethyl acetate = 10:1) to afford **1** (320mg).
^{1}HNMR (400 MHz, $CDCl_3$) δ 7.32-7.34 (m, 1H), 6.47-6.49 (d, *J* = 8 Hz, 2H), 4.58-4.66 (m, 2H), 1.37 (m, 12H).

Compound 2. A mixture of compound **1** (120 mg) and $LiAlH_4$ (41 mg) in tetrahydrofuran (10 mL) was heated to 80 °C under N_2 and stirred for 1h. Then water (50 μL), NaOH (wt10%, 50 μL), water (150 μL) were stepwise added to the solution cooled in an ice bath in order to quench the reaction. The resulting mixture was filtered by diatomite and then the filtrate was concentrated under vacuum. The residue was purified by column chromatography (silica, dichloromethane: methanol = 10: 1) to afford **2** (60 mg).
^{1}HNMR (400 MHz, $CDCl_3$) δ 7.18 (t, *J* = 16 Hz, 1H), 6.47 (d, *J* = 8 Hz, 2H), 4.53-4.62 (m, 2H), 4.25 (s, 2H), 1.37 (d, *J* = 6 Hz, 12H).

Compound 3. 200 mg of perylene tetracarboxylic dianhydride and 1g of dodecyl amine were mixed in 30 mL of methanol and refluxed for 7 hours. The resulting mixture was cooled to room temperature and acidified by 20 mL of concentrated HCl. After stirring overnight, the resulting red solid was collected by vacuum filtration through a 0.45 μm membrane filter. The solid was washed thoroughly with ethanol and distilled water until the pH of the washings turned nertral. Then the raw product containing compound **3** was used directly for the following reaction.

Compound 4. A mixture of 2,6-dimethoxybenzonitrile (150 mg) and $LiAlH_4$ (70 mg) in tetrahydrofuran (10 mL) was heated to 80 °C under N_2 and stirred for 1h. Then water (100 μL), NaOH (wt 10%, 100 μL), water (300 μL) were stepwise added to the solution cooled in an ice bath in order to quench the reaction. The resulting mixture was filtered through diatomite and then the filtrate was concentrated under vacuum. The residue was purified by column chromatography (silica, dichloromethane: methanol = 10: 1) to afford **4** (100 mg).
^{1}HNMR (400 MHz, $CDCl_3$) δ 7.00-7.04 (t, *J* = 16 Hz, 1H), 6.38 (d, *J* =12 Hz, 2H), 3.74 (s, 2H), 3.66 (s, 6H).

Compound I2/III. The mixture containing compound **3** (30 mg), compound **2/4** (30 mg) and imidazole (3 g) were heated to 140 °C and stirred for 3 hours under argon. The resulting mixture was cooled to room temperature and dispersed in 25mL of ethanol, followed by addition of 20 mL of concentrated HCl. After stirring overnight, the resulting red solid was collected by vacuum filtration through a 0.45 μm membrane filter, followed by thoroughly washing with ethanol and distilled water. The residue was purified by column chromatography (silica, chloroform: acetone =100:1) to afford **I2** (20 mg)/**III** (18 mg). The pure target compounds as obtained were confirmed by ^{1}HNMR and MALDI-TOF-MS as below.

Compound I2. ^{1}HNMR (400 MHz, $CDCl_3$): δ 8.51-8.54 (m, 4H), 8.40-8.43 (m, 4H), 7.08-7.12 (t, *J* = 16 Hz, 1H), 6.48-6.50 (d, *J* = 8 Hz, 2H), 5.51 (s, 2H), 4.51-4.54 (m, 2H), 4.17-4.20 (t, *J* = 15 Hz, 2H), 1.74-1.76 (m, 2H), 1.38-1.40 (t, *J* = 8 Hz, 6H), 1.22-1.26 (m, 18H), 0.86 (m, 3H). MALDI-TOF-MS: (M+ Na^+) = 787.3 (See Figures S12 and S13).

Compound III. ^{1}HNMR (400 MHz, $CDCl_3$): δ 8.68-8.71 (m, 4H), 8.61-8.63 (m, 4H), 7.15-7.19 (t, 1H), 6.53-6.55 (d, *J* = 8 Hz, 2H), 5.52 (s, 2H), 4.18-4.22 (m, 2H), 3.77 (s, 6H), 1.77 (m, 2H), 1.51-1.54 (t, *J* = 12 Hz, 6H), 1.25 (m, 18H), 0.86 (m, 3H). MALDI-TOF-MS: (m/z) = 708.5 (See Figures S17 and S18).

Compound IV. A mixture of 50 mg of perylene tetracarboxylic dianhydride, 30 mg of compound **4**, and 3g of imidazole were heated to 140 °C and stirred for 3 hours under argon. The reaction mixture was cooled to room temperature and dispersed in 25 mL of ethanol, followed by addition of 20 mL of concentrated HCl. After stirring overnight, the resulting red solid was collected by vacuum filtration through a 0.45 μm membrane filter, followed by thoroughly washing with ethanol and distilled water. The residue was purified by column chromatography (silica, chloroform: acetone =100:1) to afford **IV** (12 mg). The pure target compound as obtained was confirmed by high temperature ^{1}HNMR and MALDI-TOF-MS as below.
^{1}HNMR (500 MHz, 100 °C, 1,1,2,2-Tetrachloroethane-d_2): δ 8.65-8.67 (m, 4H), 8.60-8.62 (m, 4H), 7.17 (m, 2H), 6.54-6.56 (d, *J* = 8 Hz, 4H), 5.52 (s, 4H). MALDI-TOF-MS: (m/z) = 690.6 (See Figures S19 and S20).

Self-assembly of molecules I-IV into microribbons.

The **I1** microribbons were self-assembled by placing a vial containing 0.5 mL chloroform solution (0.15 mM) of **I1** into a closed jar (25 mL) containing 5 mL ethanol. The slow diffusion of ethanol in the closed jar into chloroform solution in the vial gave rise to the mircoribbons 3 days later. The **I2** microribbons were fabricated by injecting a chloroform solution (2.5 mM, 1 mL) into 10 mL ether (poor solvent) in a test tube followed by a full mixing and aging for 5 days. The self-assembly of molecule **II1** was proceeded by carefully adding 5 mL of ethanol (poor solvent) onto an *o*-dichlorobenzene solution of **II1** (2 mM, 1 mL) in a test tube or vial followed by aging for 2 days. The microribbons from **II2** and **IV** were assembled by heating 30 mL *o*-dichlorobenzene solution of the corresponding compound (0.15 mM) to 140 ℃ and then allowing the mixture to cool to room temperature followed by 3 days of aging. The **III** microribbons were assembled by carefully adding 10 mL acetone onto a chloroform solution of **III** (0.14 mM, 1 mL) in a test tube or vial followed by 2 days of aging. The assembled microribbons suspended in solution can be easily transferred onto various substrates (e.g., silica, copper grid, glass slide) by simple drop-casting for different characterizations.

Structural and optical characterizations of the assembled microribbons.

The selected area electron diffraction (SAED) patterns of the microribbons were obtained on FEI TecnaiG2 T20 (120 kV). The X-ray diffraction of the microribbons were measured by a PANalytical X'Pert PRO instrument (40 kV, 200 mA) operated in the 2θ range from 2° to 30°. The fluorescent spectra of the microribbons was collected with an Olympus FV1000 inverted confocal laser scanning microscopy (CLSM) using the lambda-mode option. The emission profiles were recorded at a resolution of 1 nm in the range from 550 to 775 nm. The raw data recorded by means of the lambda-mode were processed by Olympus Fluoview software.

Electro-driven morphological changes measurements.

SEM measurements were performed on a HITACHI S-4800 field-emission scanning electron microscope where the accelerating voltage and the current were set as 10 KV and 10 μA, respectively. Transmission electron microscopy (TEM) measurements showing the morphological changes were performed with a JEOL JEM-2010 (120 kV). The samples for SEM and TEM measurements were prepared by drop-casting the suspending microribbons in ethanol onto a copper grid followed by sputtering Pt on the surface. The Pt sputtering was performed on a Leica EM SCD 500 instrument where the current and time were set as 15 mA and 120 s, respectively. The thickness of the sputtered Pt layer was about 3 nm.

Reduction of the microribbons by hydrazine.

The samples were prepared by drop-casting the suspending microribbons in ethanol onto a copper grid. Then a vial containing the copper grids were put into a closed jar (20 mL) containing 5 mL hydrazine under argon. The microribbons on the copper grids were reduced by hydrazine vapor in the closed jar. After 3 hours, the copper grids were taken out of the jar for SEM measurements. Electron spin resonance (ESR) measurements were performed with a Bruker ESP-300E spectrometer under the settings of center field, 3480.00 G, microwave frequency, 10.0 GHz, and microwave power, 10.3 mW.

Simulated molecular packing in the assembled microribbons.

The lattice parameters of a, b, c, and γ were deduced from SAED and XRD results of the microribbons. Simulated crystal packing was verified by comparing calculated XRD patterns with the experimental XRD results. Before crystal packing simulation, the geometry structure of corresponding molecules was optimized by using density functional theory (DFT) calculation (Dmol3 package). The basis set of DFT calculation adopted DND with value of 3.5. The Monkhorst-Pack k-point mesh of 1 × 1 × 1 was used to conduct the geometry optimization calculations. The convergence tolerances of energy, force and displacement for the optimized calculation were 2.0×10^{-5} Ha per atom, 0.004 Ha $Å^{-1}$, and 0.005 Å, respectively. The wider Monkhorst-Pack k-point mesh was tested and little change on the structure and free energy of built model was observed, confirming the high accuracy of present calculations.

Table.

Table S1. The summary of deduced lattice parameters of the microribbons based on the XRD results and SAED patterns described in Figure S3.

	a	**b**	**c**	**α**	**β**	**γ**
I1	4.6 Å	9.9 Å	20.2 Å	90°	90°	93°
I2	4.3 Å	9.7 Å	21.5 Å	90°	90°	88°
II1	4.6 Å	8.7 Å	43.6 Å	90°	90°	77°
II2	16.8 Å	4.7 Å	34.9 Å	90°	110°	90°
III	4.3 Å	8.5 Å	21.9 Å	90°	90°	77°
IV	4.7 Å	7.7 Å	20.3 Å	90°	90°	68°

Other Supporting figures.

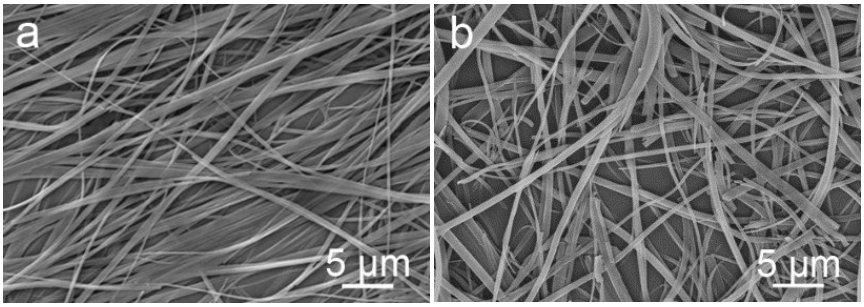

Figure S1. SEM images of the microribbons assembled from **I2** (a) and **II2** (b).

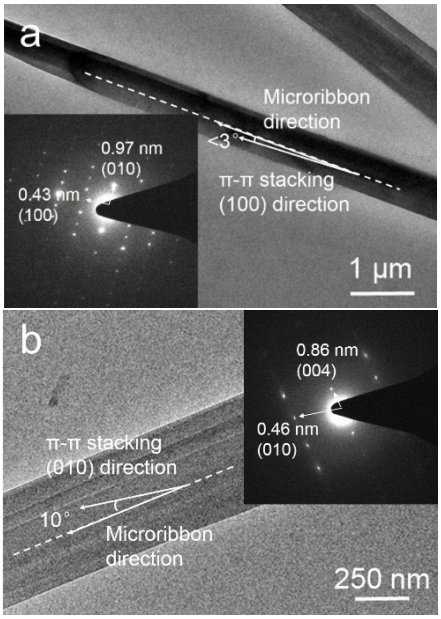

Figure S2. Typical SAED patterns of the microribbons from **I2** (a) and **II2** (b), showing that the angular offset between the π-stacking direction and the long axis of the microribbon.

.

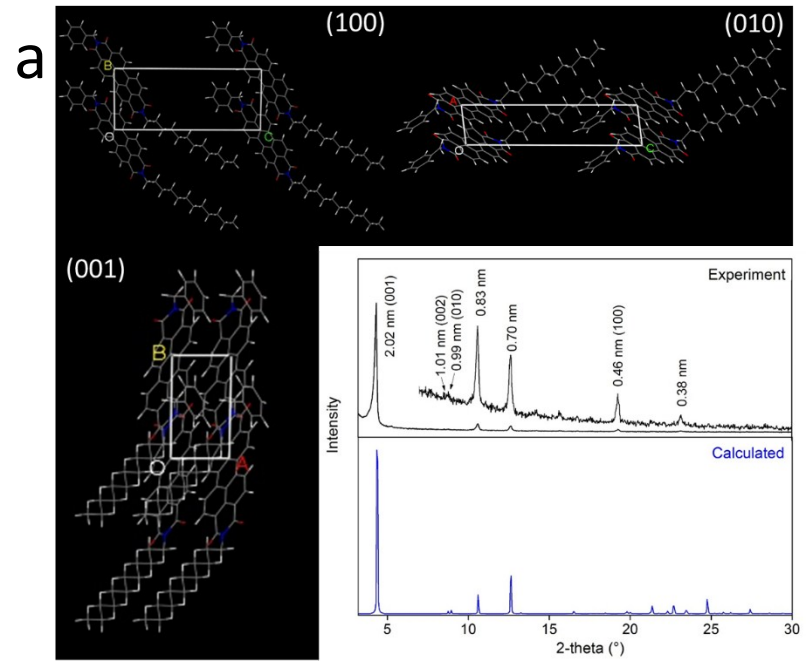
a
(100)
(010)
(001)
B
C
A
Experiment
2.02 nm (001)
1.01 nm (002)
0.99 nm (010)
0.83 nm
0.70 nm
0.46 nm (100)
0.38 nm
Intensity
Calculated
5
10
15
20
25
30
2-theta (°)

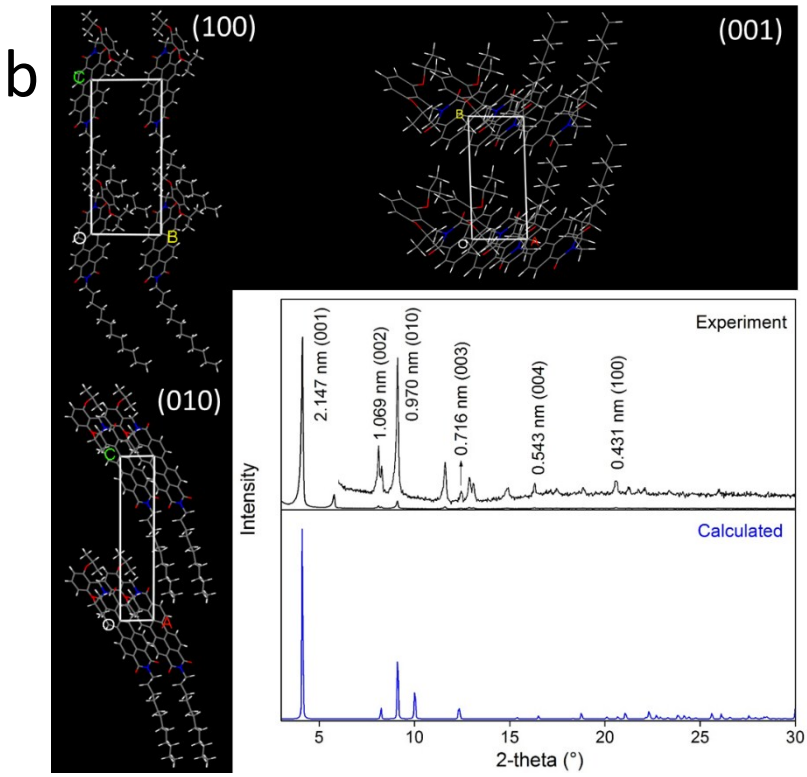
b
(100)
(001)
(010)
C
B
A
Experiment
2.147 nm (001)
1.069 nm (002)
0.970 nm (010)
0.716 nm (003)
0.543 nm (004)
0.431 nm (100)
Intensity
Calculated
5
10
15
20
25
30
2-theta (°)

c

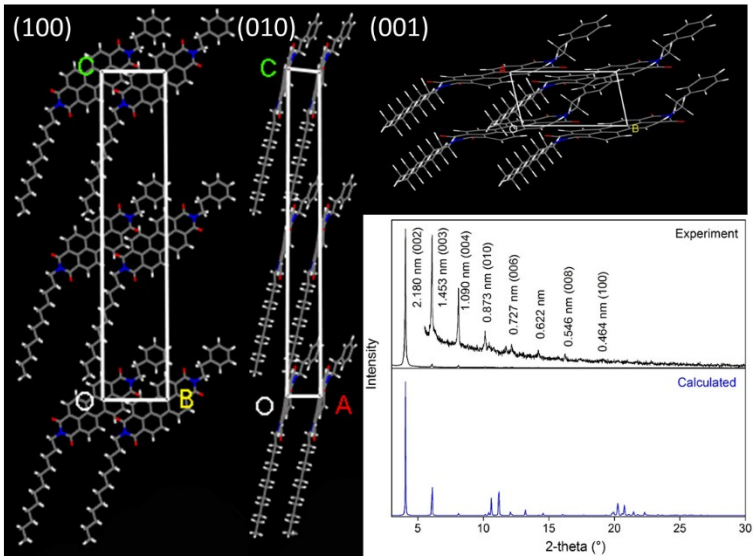
(100)
(010)
(001)
C
C
B
A
Experiment
2.180 nm (002)
1.453 nm (003)
1.090 nm (004)
0.873 nm (010)
0.727 nm (006)
0.622 nm
0.546 nm (008)
0.464 nm (100)
Intensity
Calculated
5
10
15
20
25
30
2-theta (°)

d

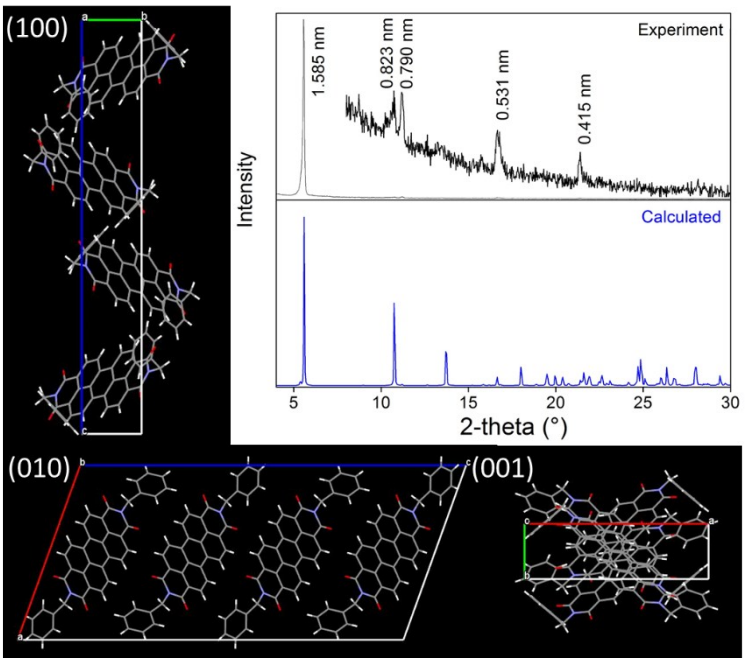
(100)
(010)
(001)
Experiment
1.585 nm
0.823 nm
0.790 nm
0.531 nm
0.415 nm
Intensity
Calculated
5
10
15
20
25
30
2-theta (°)

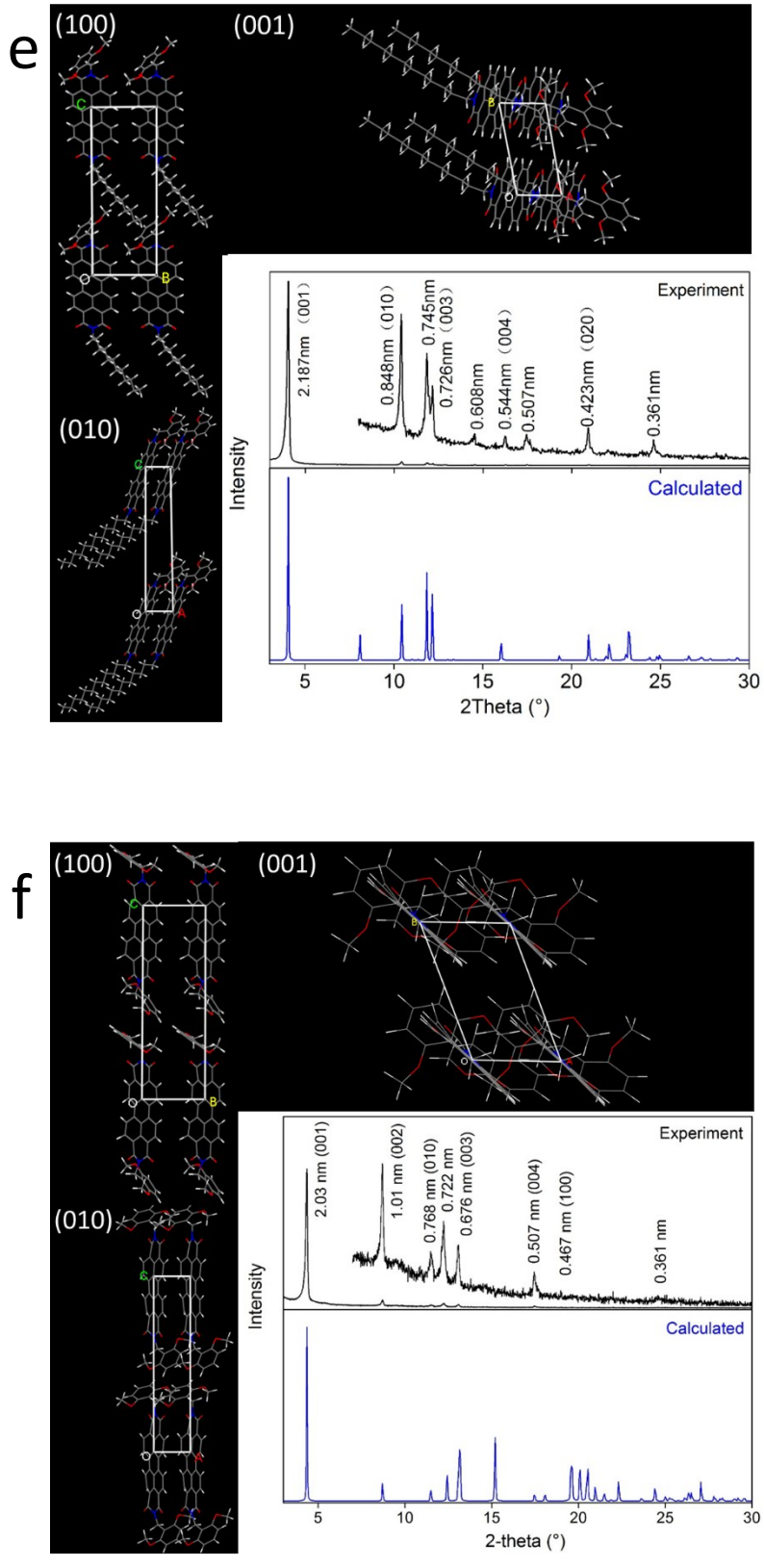

Figure S3. The molecular arrangement viewed from (100), (010), (001) faces and the calculated XRD patterns (blue lines) based on simulated crystal packing of **I1** (a), **I2** (b), **II1** (c), **II2** (d), **III** (e), and **IV** (f). For comparison, the experimental XRD results of the corresponding microribbons are also provided (black lines).

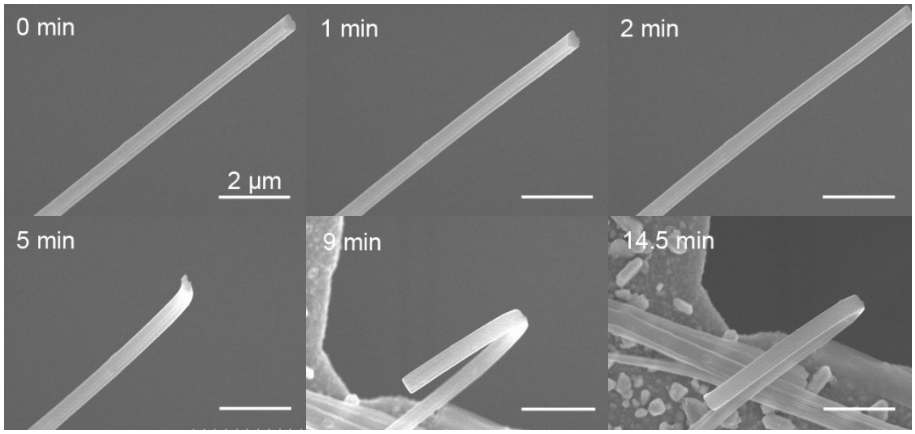

Figure S4. The time-dependent morphological changes of a typical microribbon assembled from **I2** when exposed to the scanning electron beam during SEM measurements.

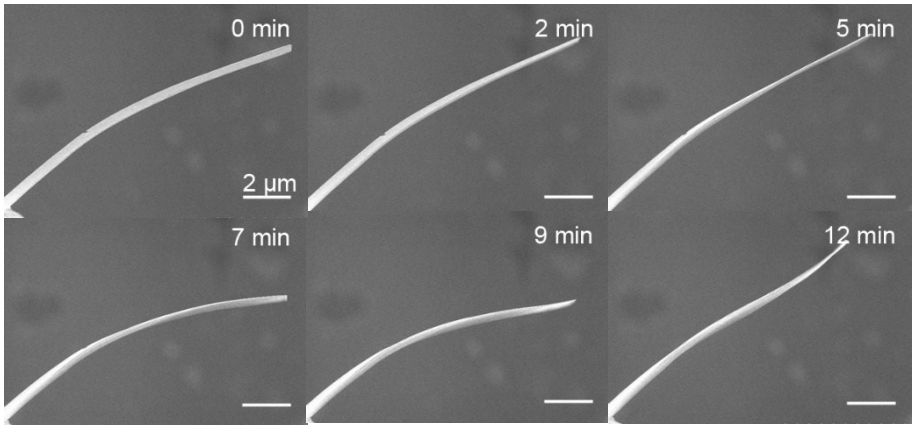

Figure S5. The time-dependent profile of morphological changes of a typical microribbon assembled from **II2** when exposed to the scanning electron beam during SEM measurements.

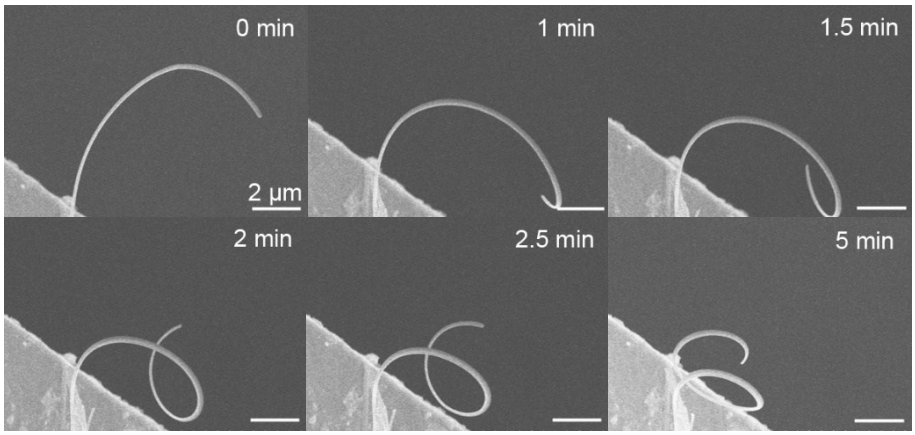

Figure S6. The time-dependent morphological changes of a relatively narrow microribbon (about 300 nm in width) assembled from **IV** when exposed to the scanning electron beam during SEM measurements.

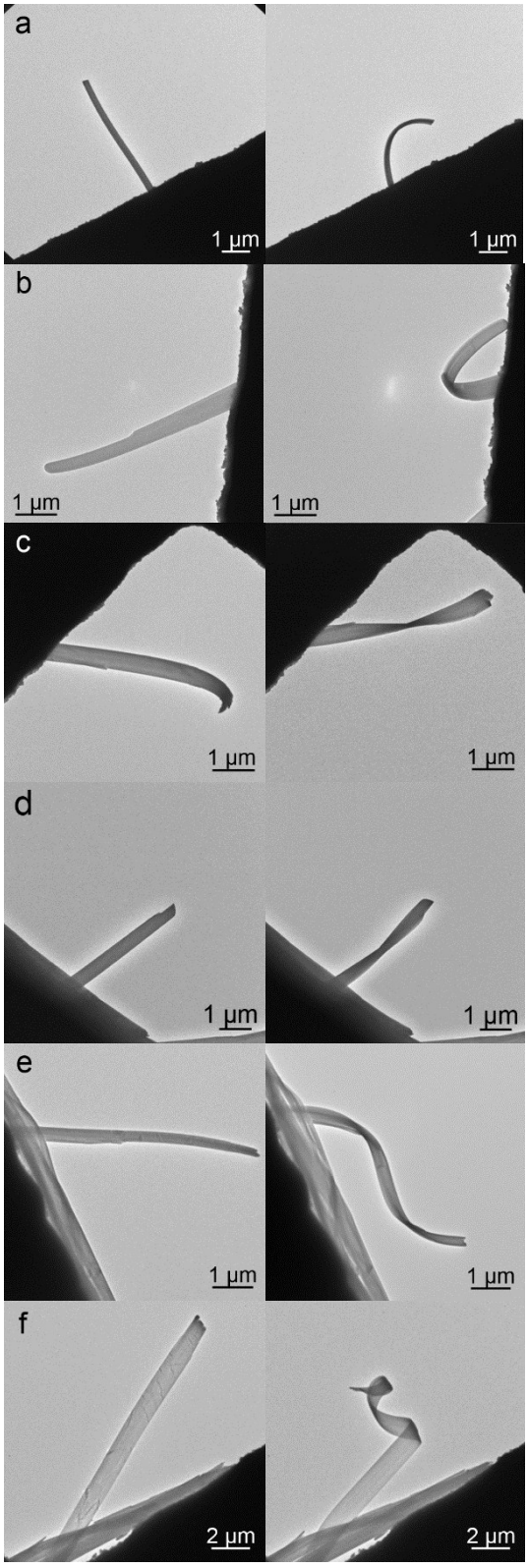

Figure S7. TEM images of the suspended microribbons assembled from **I1** (a), **I2** (b), **II1** (c), **II2** (d), **III** (e), and **IV** (f), showing their quick morphological changes upon tens of seconds of constant electron bombardment.

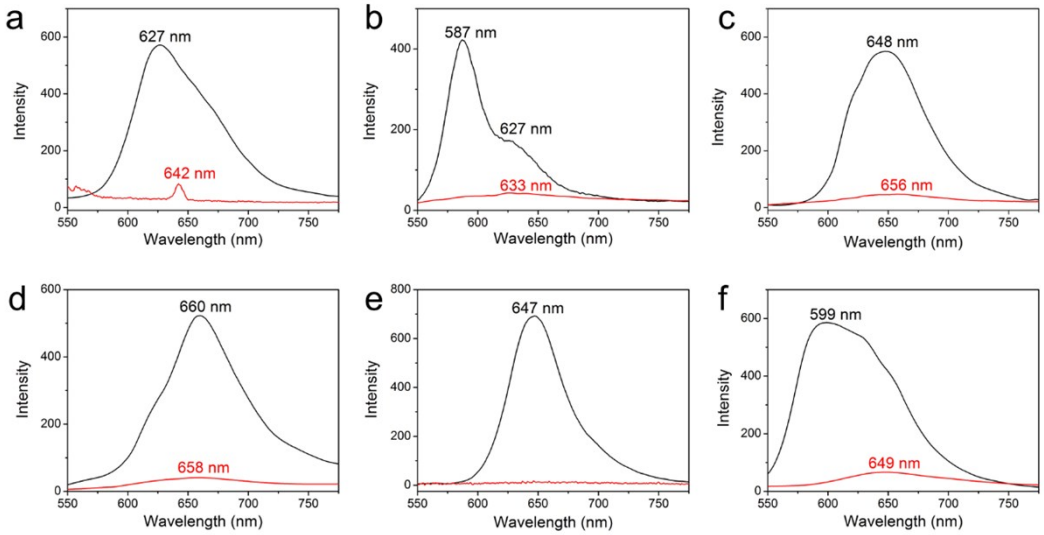

Figure S8. Fluorescence spectra of the microribbons from **I1** (a), **I2** (b), **II1** (c), **II2** (d), **III** (e), and **IV** (f) before (black lines) and after (red lines) the electron beam irradiation, which were obtained on a CLSM (λ_{ex}= 515 nm).

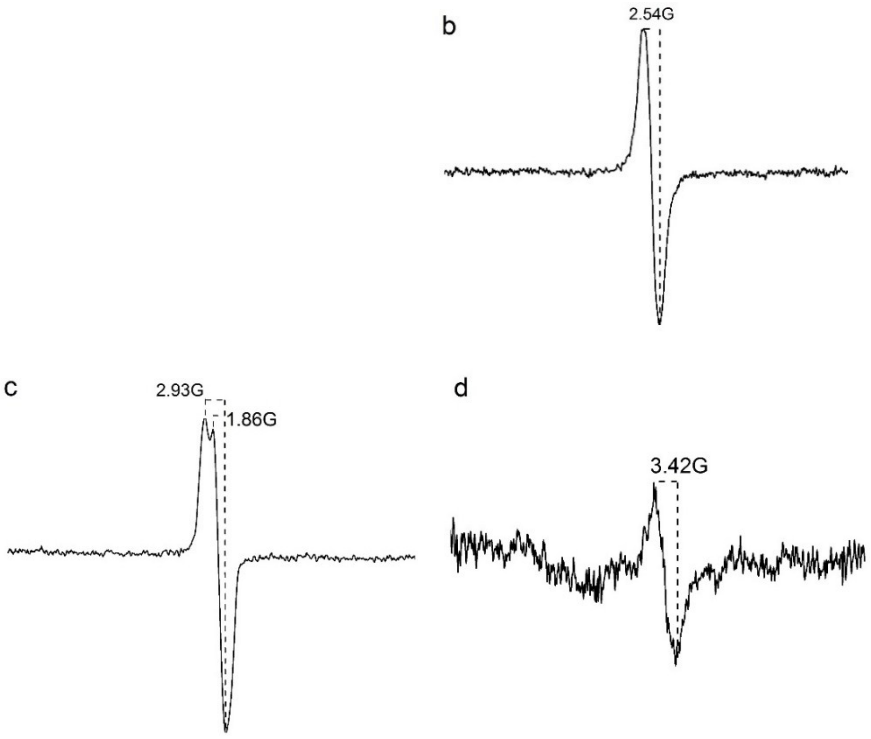

Figure S9. EPR spectra of the corresponding microribbons from **I1** (a), **II1** (b), **III** (c), and **IV** (d) when exposed to the hydrazine vapor under argon for 2 h.

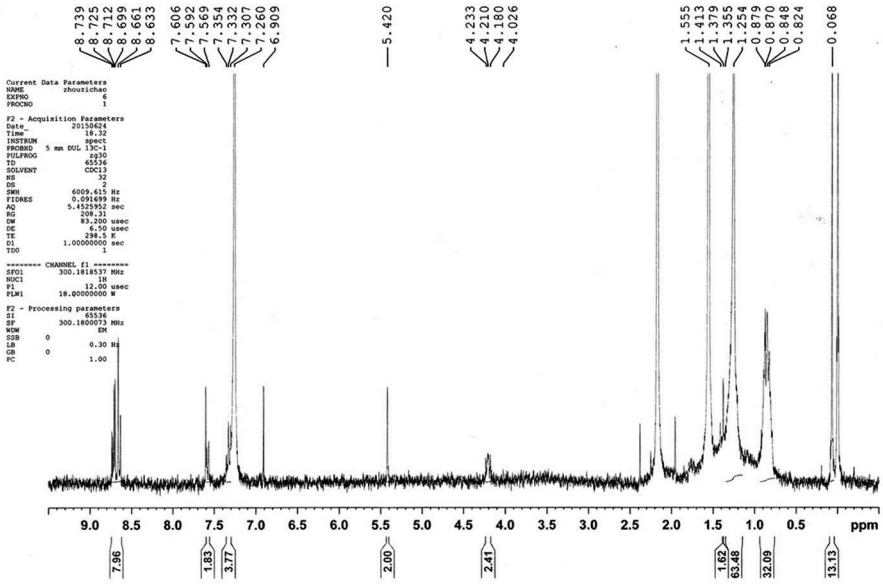

Figure S10. [1]HNMR spectrum of compound **I1**.

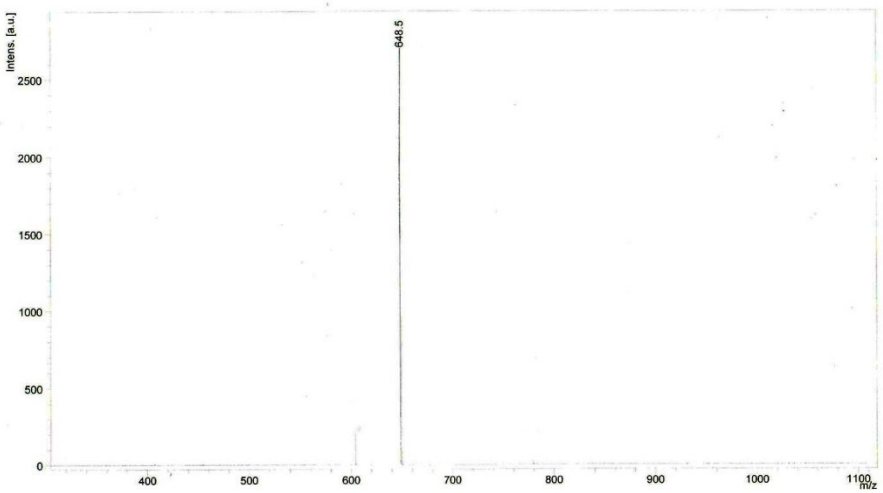

Figure S11. MALDI-TOF-MS spectrum of compound **I1**.

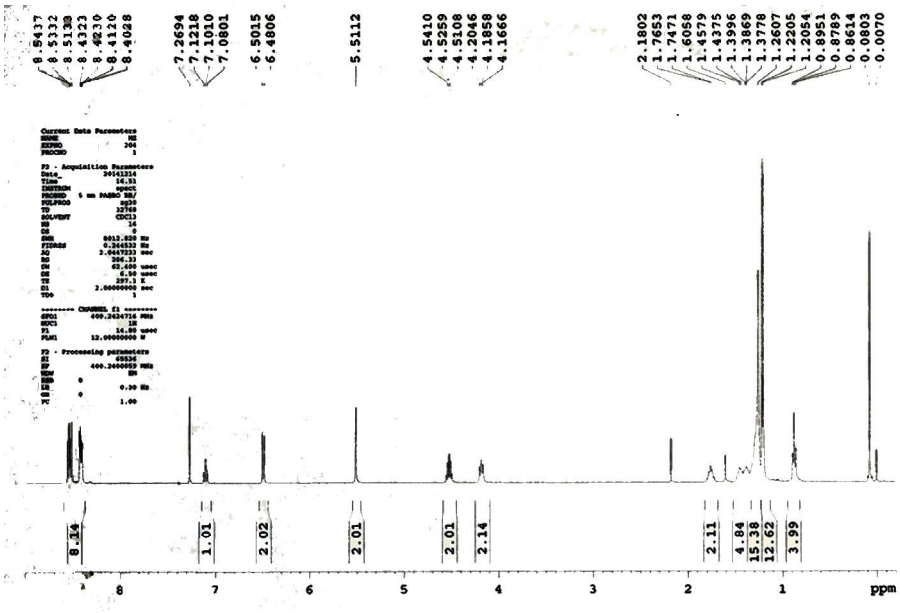

Figure S12. [1]HNMR spectrum of compound **I2**.

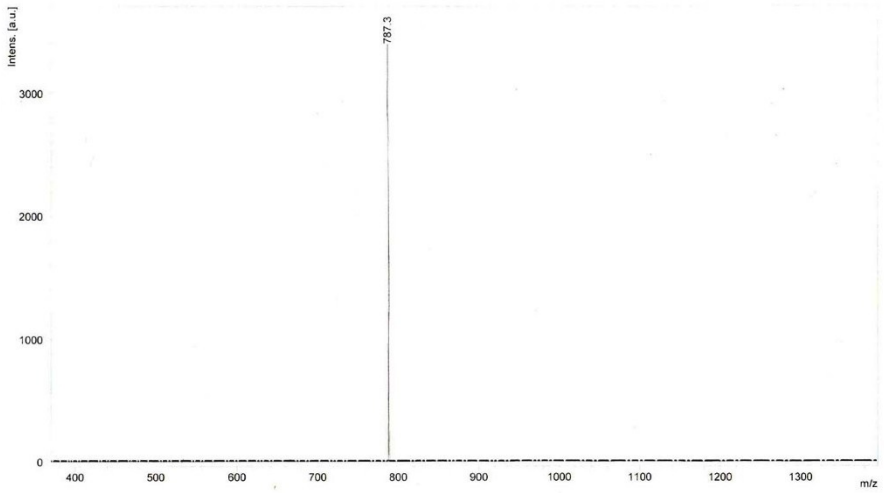

Figure S13. MALDI-TOF-MS spectrum of compound **I2**.

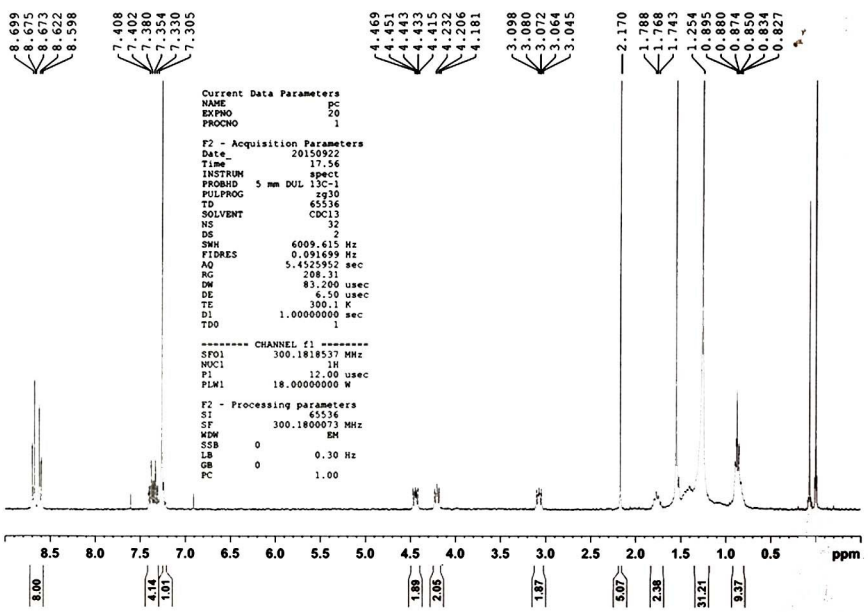

Figure S14. [1]HNMR spectrum of compound **II1**.

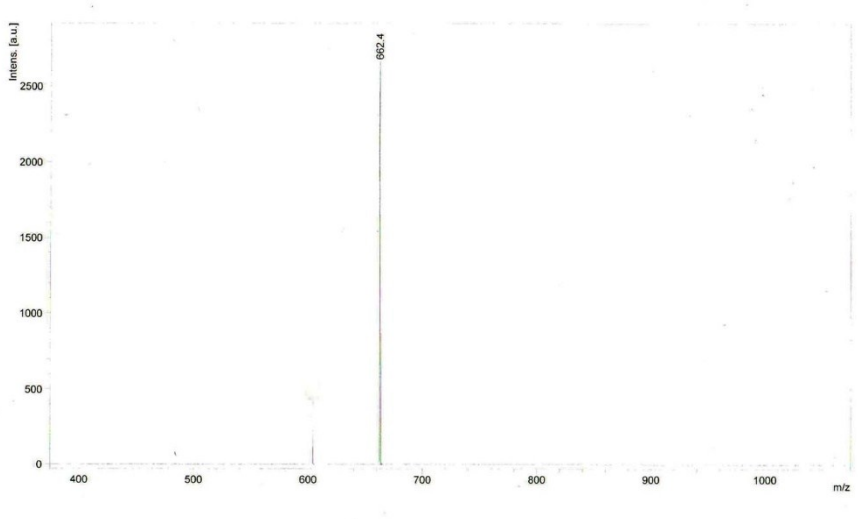

Figure S15. MALDI-TOF-MS spectrum of compound **II1**.

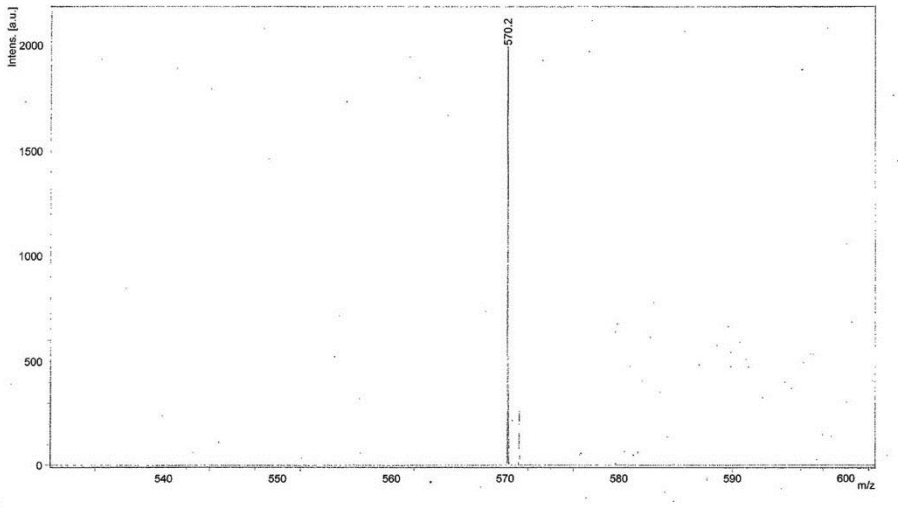

Figure S16. MALDI-TOF-MS spectrum of compound **II2**.

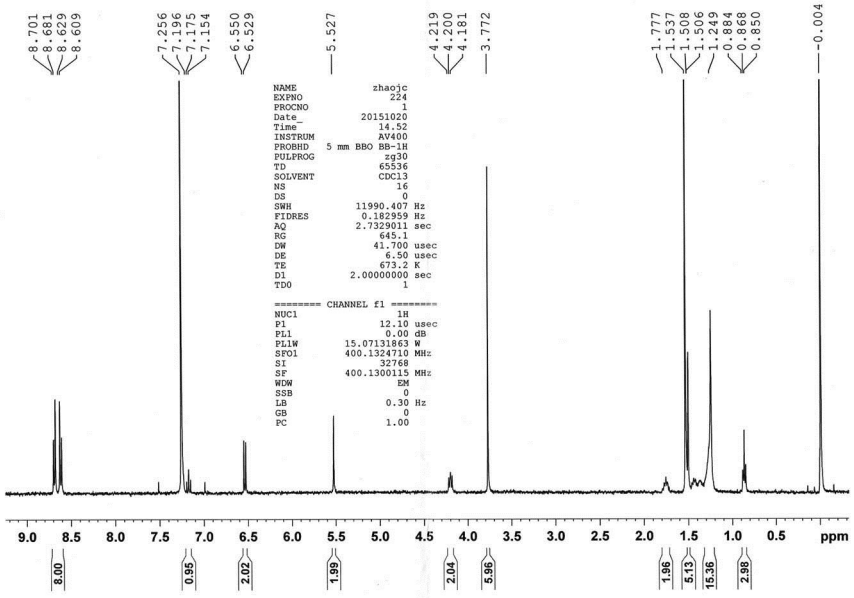

Figure S17. [1]HNMR spectrum of compound **III**.

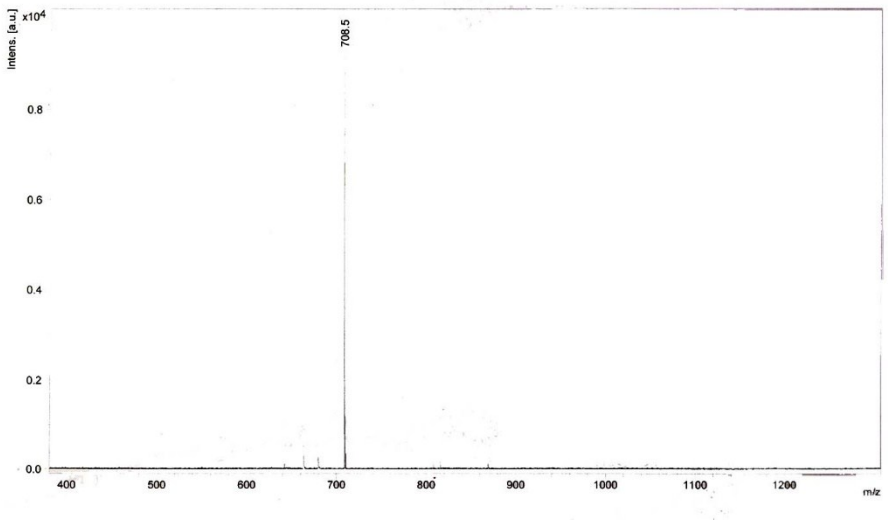

Figure S18. MALDI-TOF-MS spectrum of compound **III**.

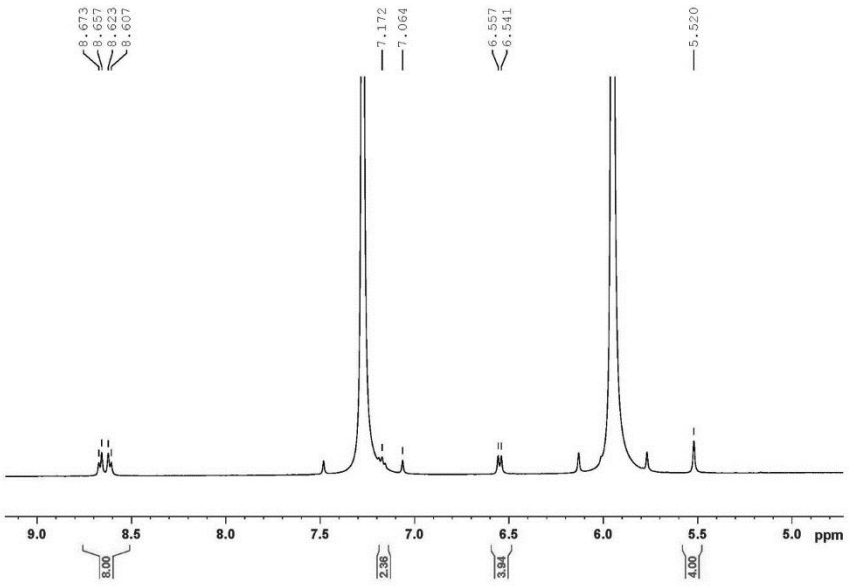

Figure S19. [1]HNMR spectrum of compound **IV**.

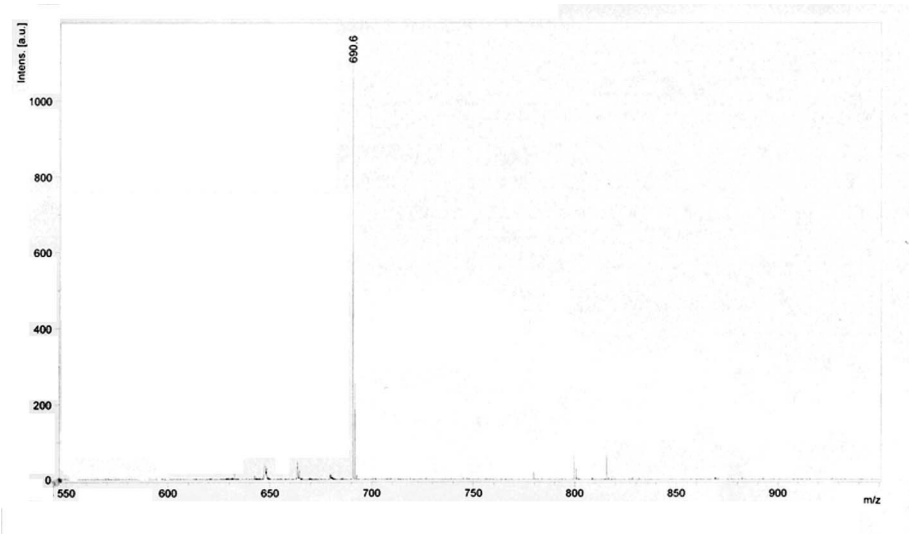

Figure S20. MALDI-TOF-MS spectrum of compound **IV**.

Reference.

[1] Che, Y.; Yang, X.; Liu, G.; Yu, C.; Ji, H.; Zuo, J.; Zhao, J.; Zang, L.; J. Am. Chem. Soc. **2010**, *132*, 5743-5750.